Research Article

Rapid Communications in Mass Spectrometry

Received: 25 June 2015 Revised: 11 August 2015 Accepted: 10 September 2015 Published online in Wiley Online Library

Rapid Commun. Mass Spectrom. **2015**, *29*, 2293–2301
(wileyonlinelibrary.com) DOI: 10.1002/rcm.7395

Phenyl group participation in rearrangements during collision-induced dissociation of deprotonated phenoxyacetic acid

Luc M. LeBlanc, Andrew M. J. Crowell, J. Stuart Grossert and Robert L. White*

Department of Chemistry, Dalhousie University, 6274 Coburg Road, PO Box 15000, Halifax, Nova Scotia, B3H 4R2, Canada

RATIONALE: The identification of trace constituents in biological and environmental samples is frequently based on the fragmentation patterns resulting from the collision-induced dissociation (CID) of gas-phase ions. Credible mechanistic characterization of fragmentation processes, including rearrangements, is required to make reliable assignments for structures of precursor and product ions.

METHODS: Mass spectra were collected using both ion trap and triple quadrupole mass spectrometers operating in the negative ion mode. Precursor ion scans and CID of ions generated in-source were used to establish precursor-product ion relationships. Density functional theory (DFT) computations were performed at the MP2/6-311++G(2d,p)//B3LYP/6-31++G(2d,p) level of theory.

RESULTS: Product ions at *m/z* 93 and 107 obtained upon CID of phenoxyacetate were attributed to phenoxide and *o*-methylphenoxide, respectively. An isotopic labeling experiment and computations showed that the phenoxide ion was formed by intramolecular displacement with formation of an α-lactone and also by a Smiles rearrangement. Rearrangement of phenoxyacetate via the ion-neutral complex formed in the α-lactone displacement pathway gave the isomeric *o*-hydroxyphenylacetate ion which yielded *o*-methylphenoxide upon decarboxylation. Computations provided feasible energetics for these pathways.

CONCLUSIONS: Previously unrecognized and energetically favorable rearrangements during the collision-induced fragmentation of phenoxyacetate have been characterized using isotopic labeling and DFT computations. Notably, the phenyl substituent plays an indispensable role in each rearrangement process resulting in multiple pathways for the fragmentation of phenoxyacetate. Copyright © 2015 John Wiley & Sons, Ltd.

Phenoxyacetic acid (**1**, $PhOCH_2CO_2H$) provides the common structural framework found in the well-known phenoxy acid herbicides,[1] certain fibrate drugs used to treat hyperlipidemia,[2] and efaproxiral, a drug candidate enhancing radiation therapy of brain metastases.[3] When subjected to collision-induced dissociation (CID), the deprotonated phenoxycarboxylic acids yield a phenoxide ion as the major product ion. This characteristic fragmentation process has served as a favorable transition for quantitative selective reaction monitoring (SRM) determinations of phenoxy acids in biological[4–6] and environmental[7–10] samples.

An intramolecular nucleophilic displacement reaction yielding an α-lactone as the neutral product (e.g., Scheme 1: **1a** ⟶ PhO^- + α-lactone) has been suggested as a possible mechanism for the formation of the phenoxide product ion from deprotonated phenoxy acid herbicides.[11] This α-lactone-displacement proposal is mechanistically equivalent to the lowest energy fragmentation process of monochloroacetate ($ClCH_2CO_2^-$) characterized by mass spectral[12,13] and computational[14,15] investigations.

On the other hand, several previous studies have recognized the reaction of a nucleophilic/basic anionic center in a gas-phase anion with a phenyl substituent in the structure. Notable examples are the Smiles rearrangement[16–20] (e.g., Scheme 1: **1a** ⟶ **spiro-1a** ⟶ **2a**) and *ortho* cyclization.[19,21] For a series of phenoxyalkoxide ions [$PhO(CH_2)_nO^-$, n = 2–4],[17,19,20] these processes were competitive with intramolecular displacements yielding cyclic ethers. Overall, the importance of the Smiles and *ortho* cyclization processes in the fragmentation of phenoxyalkoxide ions indicated the possibility of alternative mechanisms to the α-lactone-displacement pathway for the formation of the phenoxide ion from the analogous phenoxy carboxylic acids.

Furthermore, CID of phenoxyacetate,[12,22] *p*-chlorophenoxyacetate[23] and deprotonated efaproxiral[6] gave a second product ion which was in each case attributed to decarboxylation. The structures of the product ions were assigned as the corresponding aryloxymethanide ions (ArylO–CR_2^-, R = H or Me) consistent with heterolytic cleavage of the C_α–CO_2^- bond.[6,12,22] However, the analogous methoxymethanide ion (CH_3O–CH_2^-) has been considered to be short-lived and unstable with respect to electron detachment,[13] and very minor or undetectable amounts were formed upon CID of methoxyacetate ($CH_3OCH_2CO_2^-$).[12,13,24,25]

While heterolytic cleavage of the C_α–CO_2^- bond by decarboxylation has been recognized as a strategy for generating carbanions of specific structures,[26–28] feasible rearrangement

* *Correspondence to*: R. L. White, Department of Chemistry, Dalhousie University, 6274 Coburg Road, PO Box 15000, Halifax, Nova Scotia, B3H 4R2, Canada.
E-mail: robert.white@dal.ca

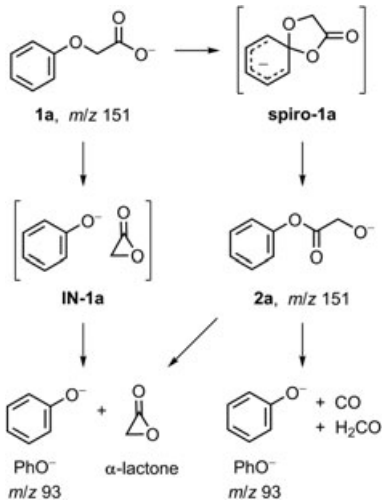

Scheme 1. Alternative pathways for the formation of the phenoxide ion (PhO^-) from phenoxyacetate (**1a**): either by intramolecular displacement and dissociation of an ion-neutral complex (**IN-1a**) or by cleavage of deprotonated phenyl glycolate (**2a**), derived from **1a** by a Smiles rearrangement.

processes prior to decarboxylation have been documented for the fragmentation of 1-bicyclo[1.1.1]pentanecarboxylate ($HC(CH_2)_3CCO_2^-$)[29] and dihydrocinnamate ($PhCH_2CH_2CO_2^-$).[30] For dihydrocinnamate, the phenyl substituent facilitated the rearrangement. In both instances, direct decarboxylation would have yielded an unstabilized alkyl carbanion ($HC(CH_2)_3C^-$ and $PhCH_2CH_2^-$, respectively), whereas decarboxylation of the rearranged ions generated stabilized product ions and required a lower input of energy.

In addition to the α-lactone-displacement and direct decarboxylation pathways, the evidence provided in the present study also supports the participation of two previously unrecognized rearrangements of phenoxyacetate upon CID. It is noteworthy that the phenyl substituent participates in each rearrangement. Overall, the fragmentation of phenoxyacetate to two product ions was shown by isotopic labeling and computed energetics to proceed via multiple pathways.

EXPERIMENTAL

Chemicals

Phenoxyacetic acid labeled with ^{18}O was prepared by adding phenoxyacetyl chloride (28 μL, 0.2 mmol) to a solution of $H_2^{18}O$ (9 μL, 0.5 mmol, 97 atom % ^{18}O) in dried acetonitrile (1 mL).[31] After 5 days at room temperature, the solvent was removed by rotary evaporation; the residue was recrystallized from water, yielding phenoxy[carboxyl-^{18}O] acetic acid (24 mg, mp 99–100°C) as a mixture of isotopologues ($^{16}O_2$:$^{16}O^{18}O$:$^{18}O_2$; 21:52:31).[32] All other compounds were obtained from Sigma-Aldrich (Oakville, ON, Canada).

Mass spectrometry

Samples were dissolved at 1 or 0.1 mg/mL in MeOH or MeOH/H_2O (1:1 v/v) and introduced into the electrospray ionization (ESI) source by flow injection using MeOH or MeOH/H_2O (1:1 v/v) at 1.2 mL/h. Negative ion mass spectra and CID spectra were acquired on Thermo-Finnigan LCQ Duo ion trap, Micromass Quattro and Waters Quattro LC triple quadrupole mass spectrometers. The ESI needle in the ion trap instrument was set at 4000 V and the capillary was maintained at 200°C. For the triple quadrupole mass spectrometers, the electrospray needle was set at 3000 V, the source cone voltage was varied from 10–35 V. Collision energies for CID experiments ranged from 15–30% (arbitrary units of the Xcalibur software) in the ion trap instrument (helium collision gas) and from 5–30 eV (laboratory frame, argon collision gas) in the triple quadrupole mass spectrometers. Precursor-product ion relationships were established using CID of in-source generated ions in addition to precursor-ion scans.

Computational methods

Quantum mechanical calculations were performed using the Gaussian 09 software package.[33] High levels of theory (i.e., using flexible enough basis sets) were used to get an accurate description of the electron densities in anions, which have diffuse character. Thus, stationary points were fully optimized in their ground states at the B3LYP/6-31++G(2d,p) level of theory.[34–36] Minima and first-order saddle-points were further characterized by their number of imaginary frequencies following normal-mode vibrational analysis, i.e., 0 and 1, respectively. First-order saddle-points were verified to connect the associated minima by stretching the bond distances along both directions of the imaginary frequency and re-optimizing to an energy minimum and/or by the use of the intrinsic reaction coordinate method.

Energies presented herein are given in terms of relative Gibbs free energies (sum of electronic and thermal free energies) which are referenced from the phenoxyacetate anion, **1a**. These are reported in kJ mol^{-1} at the MP2/6-311++G(2d,p)//B3LYP/6-311+G(2d,p) level of theory. All thermodynamic data were obtained from calculations performed in the gas phase at 298.15 K and 1.0 atm. Cartesian coordinates and energy outputs for all of the structures shown in the potential energy profiles presented can be found in the Supporting Information.

RESULTS AND DISCUSSION

The CID spectrum of phenoxyacetate (Figs. 1(A) and 1(B)) showed two major product ions, indicating the formation of the phenoxide ion (PhO^-, m/z 93) and an ion at m/z 107 by loss of carbon dioxide.[12,22] The abundance of the product ion at m/z 107 relative to that at m/z 93 was greatest in the ion trap mass spectrometer (Fig. 1(A)) and at low collision energy in the triple quadrupole mass spectrometer (Supplementary Fig. S1, Supporting Information). With increasing collision energy, the relative intensity of the ion at m/z 107 decreased: 37% (5 eV), 14% (10 eV), 5% (15 eV), 2% (20 eV) and 0.7% (≥25 eV). Further fragmentation of the ion at m/z 107 did not contribute significantly to the decrease as other product ions were very minor at high collision energy. Nevertheless, precursor-product ion determinations established that the product ions at m/z 93 and 107 were formed only from the initial phenoxyacetate ion. In

Rapid Communications in Mass Spectrometry

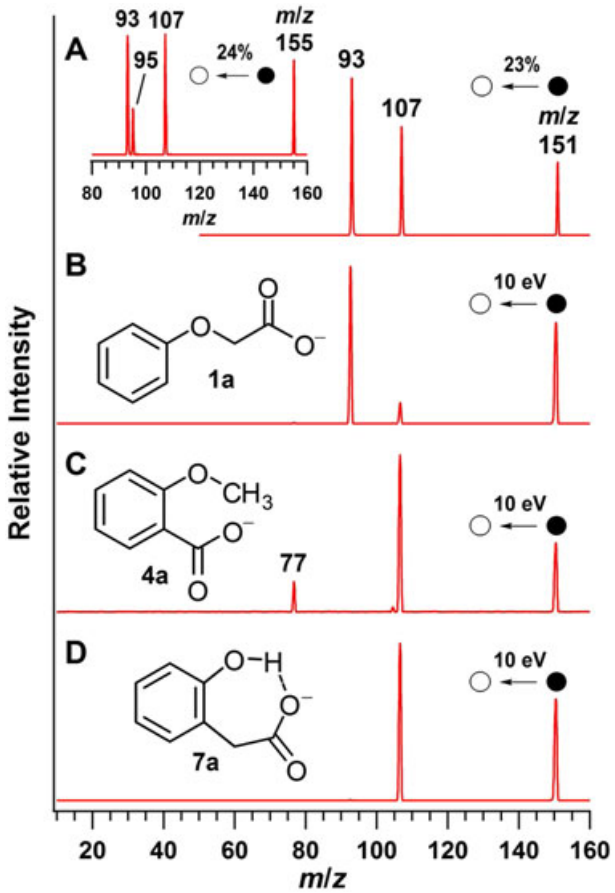

Figure 1. CID spectra of deprotonated phenoxyacetic acid (A, B), phenoxy[carboxyl-$^{18}O_2$]acetic acid (A, inset), *o*-anisic acid (C) and *o*-hydroxyphenylacetic acid (D). The spectra shown in (A) were acquired on an ion trap mass spectrometer, whereas the spectra shown in (B), (C) and (D) were collected on a triple quadrupole instrument (15 V cone).

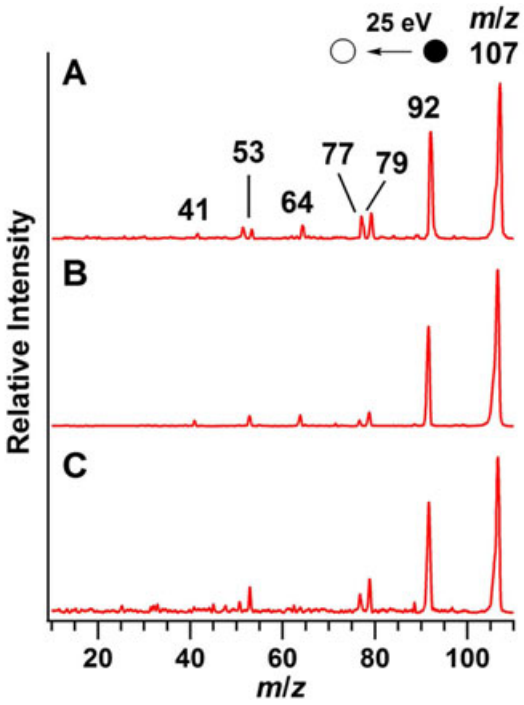

Figure 2. Tandem mass spectra of ions at *m/z* 107 derived from phenoxyacetate (A), *o*-hydroxyphenylacetate (B) and *o*-cresol (C) at 25 eV and cone voltages of 35, 35 and 15 V, respectively. The ions selected for CID in (A) and (B) were formed by decarboxylation in the source of a triple quadrupole mass spectrometer. In each spectrum, the intensity of *m/z* 10–100 has been magnified by a factor of eight.

accordance with these results, CID of the ion at *m/z* 107 generated in-source from phenoxyacetate (**1a**) yielded a product ion at *m/z* 92 and a series of lower mass, minor product ions (Fig. 2(A)). The product ions (*m/z* 75, 65, 41 and 39) generated by CID of the ion at *m/z* 93 matched those obtained at the same collision energy from deprotonated phenol (PhOH) (Supplementary Fig. S2, Supporting Information) and published data,[37] confirming PhO^- as the major product ion. The mass spectral evidence, therefore, was consistent with the formation of product ions from phenoxyacetate by two different processes.

Mechanisms of phenoxide ion (*m/z* 93) formation

In phenoxyacetate (**1a**), the aryl ring and the charged oxygen in the carboxylate group are positioned to create a favorable five-membered ring during the Smiles rearrangement, as seen previously with 2-phenoxyethoxide[17,19,20] and a deprotonated aryloxyacetamide derivative.[18] To distinguish the Smiles rearrangement from the α-lactone-displacement process (Scheme 1), a sample of phenoxy[carboxyl-^{18}O]acetic acid was prepared and subjected to ESI(–)MS/MS. The resulting CID spectrum of phenoxy[carboxyl-$^{18}O_2$]acetate (Fig. 1(A), inset; *m/z* 155) showed product ions at *m/z* 93, 95 and 107. The ion at *m/z* 107 formed by loss of $C^{18}O_2$ demonstrated that the isotopic label was present in only the carboxyl group, whereas the ion at *m/z* 95 showed retention of the label in the phenoxide ion consistent with displacement of the ether oxygen from the aryl ring by an oxygen in the carboxylate group as predicted by the Smiles rearrangement [Scheme 1: $PhOCH_2C^{18}O_2^-$ (**1a**) $\longrightarrow$ $^{18}O_2$-**spiro-1a** $\longrightarrow$ $Ph^{18}OC^{18}OCH_2O^-$ (**2a**) $\longrightarrow$ $Ph^{18}O^-$ (*m/z* 95)]. The approximately 3:1 relative abundances of the ions at *m/z* 93 and 95 indicated that both the α-lactone-displacement and the Smiles rearrangement were major fragmentation processes.

DFT computations indicated that the initial steps in the α-lactone-displacement and Smiles rearrangement pathways had barriers of 152 and 138 kJ mol^{-1}, respectively (Fig. 3). Note that a similar small energy difference was also found computationally for the analogous reactions of 2-phenoxyethoxide.[17] The products of the initial steps were only slightly more stable than the corresponding transition structure, and incremental additions of energy were needed to form PhO^- by dissociation of the ion-neutral complex **IN-1a** (Fig. 3, 32 kJ mol^{-1}) and fragmentation of deprotonated phenyl glycolate (**2a**, Fig. 4: 36, 24 or 48 kJ mol^{-1}). The similar energetics computed for these processes were consistent with the labeling results and the significant contributions of both processes to the fragmentation of phenoxyacetate. Based on the very high barrier (524 kJ mol^{-1}) computed for *ortho* cyclization and proton migration (Supplementary Fig. S4, Supporting Information), a pathway analogous to one

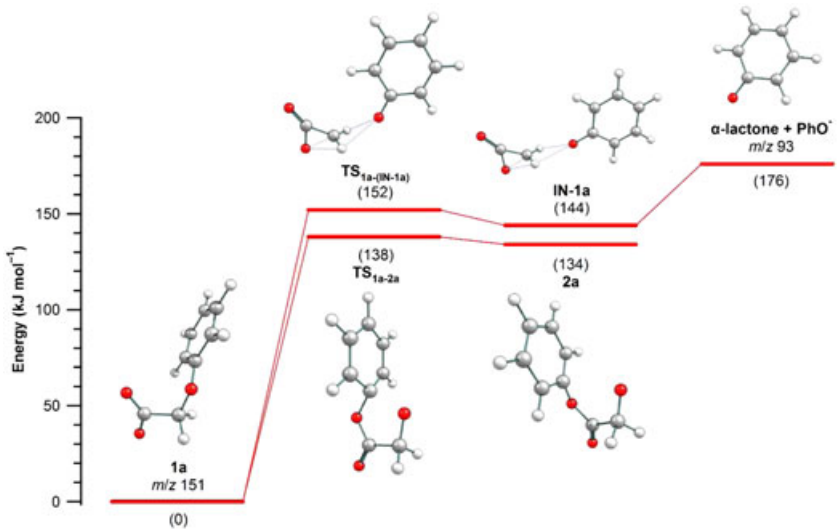

Figure 3. Potential energy profiles for the α-lactone-displacement and Smiles rearrangement processes of phenoxyacetate (**1a**) via $\mathbf{TS_{1a\text{-}(IN\text{-}1a)}}$ and $\mathbf{TS_{1a\text{-}2a}}$, respectively. Numbers in parentheses are free energies.

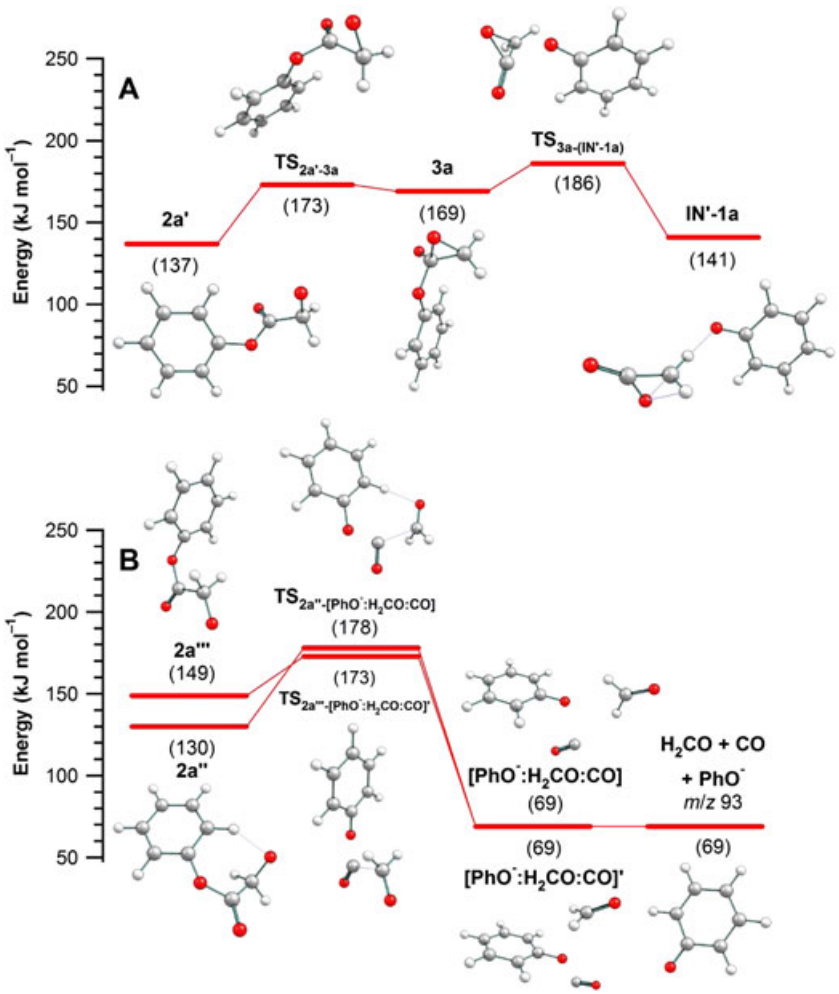

Figure 4. Potential energy profiles for the formation of PhO^- from conformations of deprotonated phenyl glycolate (**2a′**, **2a″** and **2a‴**) with concomitant formation of α-lactone (A) or carbon monoxide and formaldehyde (B). Numbers in parentheses are free energies.

Rapid Communications in Mass Spectrometry

considered for the fragmentation of deprotonated *N*-phenylbenzamides[16] was unlikely to contribute to the formation of **2a.**

In a recent computational study of the Smiles rearrangement in solution,[38] qualitative mechanistic differences were obtained when different functionals were employed. Use of the M06-2X[39] and ωB97X-D[40,41] functionals predicted a multistep mechanism incorporating a Meisenheimer adduct as a reactive intermediate, whereas, in the present work, computations based on the B3LYP functional predicted a one-step process for the Smiles rearrangement, as presented in Fig. 3. When intrinsic reaction coordinate (IRC) calculations (Supplementary Fig. S3, Supporting Information) were performed on the Smiles transition structure, $\mathbf{TS_{1a\text{-}2a}}$, located with each of the three functionals (B3LYP, M06-2X and ωB97X-D) and the 6-31++G(2d,p) basis set, only the single-step mechanism was located for the rearrangement of phenoxyacetate (**1a**) to deprotonated phenyl glycolate (**2a**). Optimization of the points on each side of the reaction path led to **1a** and **2a**, with no evidence of a Meisenheimer-type reactive intermediate. In the published computations,[38] the aryl ring had a nitro group *ortho* to the oxygen substituent and the computations were performed using an integral equation formalism polarizable continuum model (IEFPCM) for solvation (methanol). Both of these factors would likely stabilize a Meisenheimer-type intermediate enabling its characterization.

The computations also indicated that two pathways for the formation of PhO^- from deprotonated phenyl glycolate (**2a**) were energetically feasible. Formation of an α-lactone from **2a**, as suggested previously,[18] required inputs of only 36 and 17 kJ mol^{-1} for cyclization of the alkoxide ion **2a′**; subsequent breakdown of the tetrahedral intermediate **3a** to PhO^- and α-lactone, overall, was an essentially isergonic reaction (Fig. 4(A)). The alternative fragmentation leading to carbon monoxide and formaldehyde required only an additional input of 24 or 48 kJ mol^{-1} from the *anti* and *gauche* conformations **2a‴** and **2a″**, respectively, with product formation being exergonic (Fig. 4(B)).

The overall inputs of energy needed for the single-step α-lactone-displacement process and the two-step Smiles rearrangement process were equivalent (i.e., 176 vs. 186 or 173 kJ mol^{-1}). Furthermore, the barriers for the forward and reverse directions of the first step were similar (Fig. 3), and the energy needed to dissociate the ion-neutral complex in the α-lactone-displacement process corresponded to the height of the barriers for the bond cleavages in the distinct second step of the Smiles rearrangement pathway (Fig. 4). The latter, however, occurred from specific conformations that were energetically close to $\mathbf{TS_{1a\text{-}(IN\text{-}1a)}}$, making formation of phenoxyacetate by the reverse process favorable. The lack of a conformational dependence on the dissociation of the ion neutral **IN-1a** would favor the α-lactone-displacement pathway, in accord with the mass spectral observations (Fig. 1(A), inset).

Decarboxylation: a profusion of possible product ions at *m/z* 107

*Formation and rearrangement of phenoxymethanide (**1b**)*

The fragmentation process yielding the product ion at *m/z* 107 was consistent with decarboxylation, a common fragmentation process of deprotonated carboxylic acids.[25–28,30] DFT computations predicted that loss of carbon dioxide from phenoxyacetate to form phenoxymethanide [Scheme 2: $PhOCH_2CO_2^-$ (**1a**) ⟶ $PhOCH_2^-$ (**1b**) + CO_2] was a barrierless process[27,42] (Fig. 5). The input of 178 kJ mol^{-1} required for decarboxylation was equivalent to the energy requirements computed for the formation of PhO^- by either the α-lactone-displacement or the Smiles rearrangement process (Figs. 3 and 4). Thus the energetics for heterolytic C_α–CO_2^- bond cleavage for phenylacetate were in keeping with earlier proposals of methanide ion ($ArylOCR_2^-$, R = H or Me) formation by decarboxylation of α-aryloxycarboxylates ($ArylOCR_2CO_2^-$, R = H or Me)[6,12,22] and the lower relative abundance of the product ion at *m/z* 107.

The phenoxymethanide ion **1b** also has been implicated as an intermediate in the formation of the phenide ion (Ph^-, *m/z* 77) and formaldehyde from the *o*-methoxyphenide ion **4b**[22,43–45] (Scheme 2) generated by deprotonation of anisole,[44,45] decarboxylation of *o*-anisate (Fig. 1(C) and Herath *et al*.[43]) and chemical ionization of ethyl *o*-anisate.[22] Decarboxylation of phenoxyacetate with proton migration yielding the *o*-methoxyphenide ion was also energetically feasible (Supplementary Fig. S5, Supporting Information). The relative energies computed for **1b** and **4b** (Fig. 5) were consistent with the determination of the *ortho* hydrogen as the most acidic in anisole,[45] and the facility of the interconversion of **1b** and **4b** was indicated by barriers of less than 90 kJ mol^{-1} for the associated intramolecular proton transfer. The heights of these barriers closely agreed with those computed for interconversion of the analogous ions formed by decarboxylation of 2,6-dimethoxybenzoate.[43]

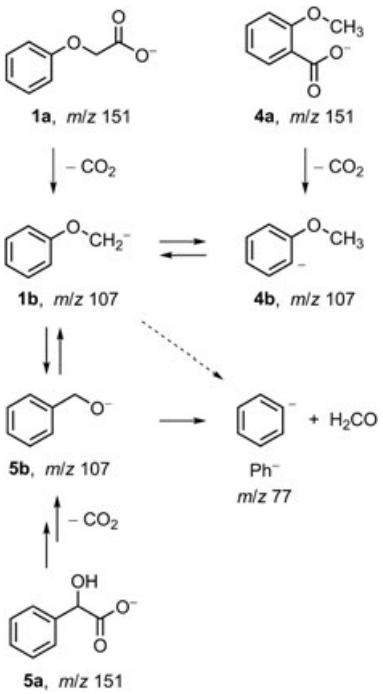

Scheme 2. Decarboxylation of phenoxyacetate (**1a**) and interconversion of phenoxymethanide (**1b**) with the isomeric *o*-methoxyphenide (**4b**) and benzyl oxide (**5b**) ions derived from *o*-anisate (**4a**) and mandelate (**5a**), respectively, and formation of the phenide ion (Ph^-) from ions at *m/z* 107.

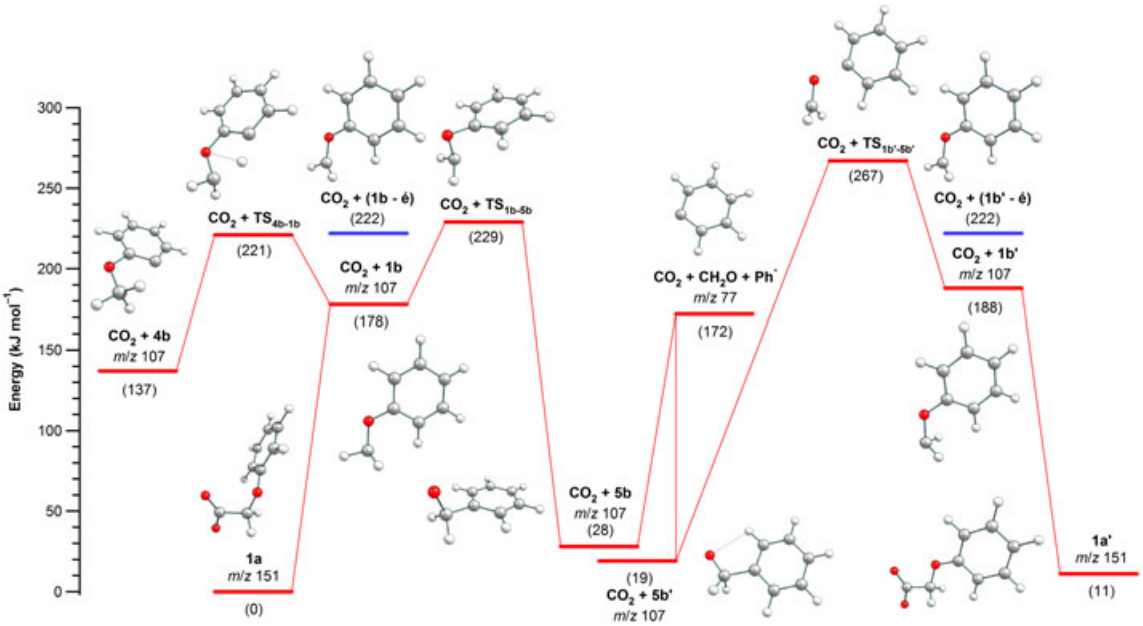

Figure 5. Potential energy profile for the generation and isomerization of ions at m/z 107 and cleavage to the phenide ion (Ph^-, m/z 77). Electron detachment energies are shown as horizontal blue lines and numbers in parentheses are free energies.

*Cleavage and stability of phenoxymethanide (**1b**)*

The computations also predicted a moderate barrier for C–O bond cleavage of the phenoxymethanide ion from conformation **1b′** derived from conformation **1a′** of phenoxyacetate (Fig. 5, 79 kJ mol^{-1}). However, the transition structure $\mathbf{TS_{1b'-5b'}}$ was connected to the benzyl oxide ion **5b′** rather than Ph^- and formaldehyde. Bond cleavage in benzyl oxide, yielding Ph^- and formaldehyde, proceeded as a barrierless and energetically viable process in keeping with the fragmentations observed in the CID spectra of ions at m/z 107 derived from anisole,[44,45] *o*-anisic acid (Supplementary Fig. S6, Supporting Information, and Herath *et al.*[43]) and ethyl *o*-anisate,[22] as well as the CID spectrum of deprotonated benzyl alcohol.[44,46] It is also noteworthy that deprotonated mandelic acid (**5a**), isomeric to phenoxyacetic acid (Scheme 2), fragmented in sequential reactions upon CID to yield product ions at m/z 107 and 77.[24] For the latter, computations supported a rearrangement of mandelate (**5a**) prior to formation of benzyl oxide (**5b**, m/z 107) by decarboxylation and subsequent cleavage to formaldehyde and Ph^- (m/z 77).

The energies computed (Fig. 5) also were consistent with the experimentally determined equilibration of phenoxymethanide (**1b**) and *o*-methoxyphenide (**4b**) ions before dissociation to formaldehyde and Ph^- (m/z 77),[44] and the formation of the phenide ion upon CID of deprotonated benzyl alcohol.[44,46] The relative barrier heights indicated that cleavage of benzyl oxide (**5b**) to formaldehyde and Ph^- was more favorable than the isomerization of **5b** to **1b**.

For gas-phase anions, the potential detachment of an electron is an important consideration for assessing ion stability. Accordingly, the energies computed for the removal of an electron from *o*-methoxyphenide (**4b**) and benzyl oxide (**5b**) were large (245 and 207 kJ mol^{-1}, respectively) and greater than the barriers for conversion of **4b** into **1b** and for fragmentation of **5b** to formaldehyde and Ph^- (Fig. 5). As deduced previously,[22] the phenoxymethanide ion **1b** was also stable. Computations indicated that the energy needed to detach an electron from conformation **1b′** was small (34 kJ mol^{-1}) and significantly less than that needed to reach the transition structure for C–O bond cleavage (Fig. 5, $\mathbf{TS_{1b'-5b'}}$), placing the viability of this often proposed cleavage reaction[22,43–45] into question.

However, computations also indicated that the barrier for a Smiles rearrangement of phenoxymethanide (**1b**) to benzyl oxide (**5b**) via the spirocyclic transition structure $\mathbf{TS_{1b-5b}}$ was energetically competitive with electron detachment, thus providing a feasible alternative route for the formation of formaldehyde and Ph^- by cleavage of **5b** derived from either **1b** or **4b**. Overall, the relationships depicted in Scheme 2 were consistent with the computational predictions (Fig. 5) and the fragmentation behavior of both *o*-anisate (**4a**, Fig. 1(C), Supplementary Fig. S6, Supporting Information, and Herath *et al.*[43]) and mandelate (**5a**).[24] Moreover, the ease of electron detachment from phenoxymethanide (**1b**) may provide a possible explanation for the decreased abundance of this product ion at higher collision energies (Fig. 1(B) and Supplementary Fig. S1, Supporting Information).

On the other hand, the reasonable energetics computed for the decarboxylation of phenoxyacetate (**1a**) to phenoxymethanide (**1b**) and the intermediate position of **1b** on the computed potential energy profile (Fig. 5) did not fully account for the decarboxylation and subsequent fragmentation processes observed for phenoxyacetate. In particular, the fragmentation behavior observed over a range of collision energies (5–30 eV) for the ion at m/z 107 generated in-source from phenoxyacetate (**1a**) (e.g., Fig. 2(A)) was markedly different from that derived from *o*-anisate (**4a**) (Supplementary Fig. S6, Supporting Information, and Herath *et al.*[43]), indicating that another pathway for the fragmentation of phenoxyacetate (**1a**) needed to be considered.

Rapid Communications in Mass Spectrometry

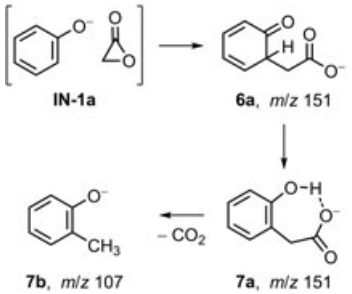

Scheme 3. Formation of *o*-hydroxyphenylacetate (**7a**) from the ion-neutral complex **IN-1a** derived from phenoxyacetate (**1a**) and subsequent decarboxylation to deprotonated *o*-cresol (**7b**), an alternative structure for the product ion at *m/z* 107.

*Rearrangement of phenoxyacetate (**1a**): a prelude to decarboxylation*

Interestingly, an analogous Smiles rearrangement of the phenoxyacetate enolate ion ($PhOCH^-CO_2H$) yielded mandelate **5a**. The barrier computed for the initial abstraction of an α-proton by the carboxylate group (Supplementary Fig. S7, Supporting Information), however, was higher than that for decarboxylation of phenoxyacetate (Fig. 5) and the sequential rearrangements were unlikely as steps in the main fragmentation pathway.

In evaluating other possible alternatives, it was noted that a competing lower energy displacement process yielding the prominent fragment ion at *m/z* 93 (Figs. 1(A), 1(B) and 4) distinguished the fragmentation behavior of phenoxyacetate (**1a**) from that of both *o*-anisate (**4a**, Fig. 1(C), Supplementary Fig. S6, Supporting Information, and Herath *et al.*[43]) and mandelate (**5a**).[24] Dissociation of the ion-neutral complex formed between PhO^- and an α-lactone (**IN-1a**) required further input of energy (Fig. 3) but recombination of phenoxide ion and the α-lactone was possible and was evaluated as an alternative (Scheme 3). Indeed, the computations (Fig. 6) indicated that *ortho* alkylation of the phenoxide ion within **IN′′-1a** and a subsequent proton transfer step regenerating the aromatic ring had barriers of only 17 and 9 kJ mol^{-1}, respectively. It was important to note that the proton transfer step was more favorable than decarboxylation of the *o*-alkylated phenoxide ion (**6a**) leading to formation of a bicyclic product ion (**9b**, Fig. 6) and other higher energy alternatives (Supplementary Fig. S8, Supporting Information). The rearranged ion **7a** corresponded to *o*-hydroxyphenylacetate, and decarboxylation was observed as the predominant process when a standard sample of *o*-hydroxyphenylacetic acid was deprotonated and subjected to CID (Fig. 1(D)). The transition structures ($\mathbf{TS_{7a\text{-}[7b:CO2]}}$ and $\mathbf{TS_{7a'\text{-}[7b:CO2]'}}$) located by the computations showed that proton transfer accompanied C_α–CO_2^- bond cleavage, a rearrangement characterized computationally for the decarboxylation of the monoanions of dicarboxylic acids.[47] The alignment of atoms in the transition structures correlated with the initial conformations **7a** and **7a′**, and the different energies of the conformations gave different heights for the barriers for decarboxylation.

An analogous pathway starting with alkylation of phenoxide at the *para* position was examined computationally (Supplementary Fig. S9, Supporting Information). While a similar low barrier for *p*-alkylation in a realigned ion-neutral complex was found, the barrier for the subsequent proton transfer step (228 kJ mol^{-1}) was much higher than the barriers in the *ortho* pathway (Fig. 6), and the *para* route is therefore less likely.

Nevertheless, an ion-neutral complex (**IN-1a**, Schemes 1 and 3) must be considered as the common precursor of both product ions formed upon CID of phenoxyacetate (Figs. 1(A) and 1(B)). At higher collision energies in the triple quadrupole mass spectrometer, the energized **IN-1a** would be more likely

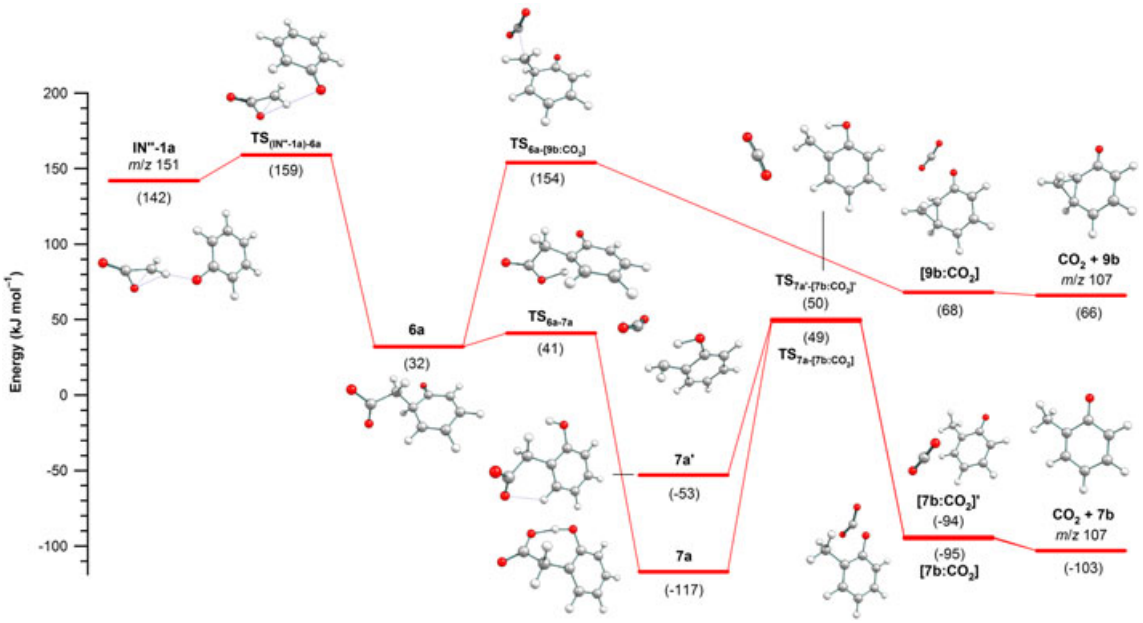

Figure 6. Potential energy profile for the rearrangement of the ion-neutral complex **IN′′-1a** to *o*-hydroxyphenylacetate (**7a**) and subsequent decarboxylation yielding *o*-methylphenoxide (**7b**) at *m/z* 107. Numbers in parentheses are free energies.

to dissociate before achieving the alignment needed for recombination by alkylation. Consequently, the yield of PhO^- (m/z 93) would increase and that of the ion at m/z 107 would decrease, in accord with the lower relative abundance observed for the ion at m/z 107 (Fig. 1(B) and Supplementary Fig. S1, Supporting Information).

Moreover, CID of the ion at m/z 107 generated in-source from *o*-hydroxyphenylacetate (**7a**) and CID of deprotonated *o*-cresol (**7b**, *o*-methylphenoxide) yielded a major product ion at m/z 92 and a series of minor product ions in common with those formed by CID of the ion at m/z 107 formed in-source from phenoxyacetate (**1a**) (Fig. 2). Formation of the ion at m/z 92 from *o*-methylphenoxide (**7b**) has been shown to proceed by loss of a methyl radical by homolytic cleavage.[44,48] Thus, both the mass spectral and computational results support rearrangement of phenoxyacetate and subsequent decarboxylation yielding **7b** as a significant product ion at m/z 107.

CONCLUSIONS

Building on previous work,[12,22] the gas-phase chemistry of phenoxyacetate, an ion of simple structure, was shown here to involve multiple fragmentation and rearrangement pathways. The two product ions at m/z 93 and 107 were each formed by two distinct pathways. The barriers computed for the α-lactone-displacement and Smiles rearrangement processes were similar and isotopic labeling demonstrated the contribution of both pathways to phenoxide ion formation. Reaction of the phenoxide ion with the neutral α-lactone in the ion-neutral complex formed by the α-lactone-displacement process yielded *o*-hydroxyphenylacetate as an intermediate on an energetically favorable route to *o*-methylphenoxide (**7b**) as a relevant product ion at m/z 107. Decarboxylation yielding the previously considered phenoxymethanide ion (**1b**)[12,22] was likely a minor process.

While the phenyl substituent stabilized charge in the product ions, it also facilitated rearrangement processes described by an energy surface with several barriers of equivalent height. Therefore, possible participation of the phenyl substituent, particularly in rearrangement processes, becomes an important consideration in the interpretation of fragmentation patterns and the assignment of structure to gas-phase ions.

Acknowledgements

We thank the Natural Sciences and Engineering Research Council of Canada (NSERC) for financial support, Dr. A. A. Doucette for the use of the Quattro LC, X. Feng for maintenance of the ion trap mass spectrometer in the MMSLab, Dr. E. A. L. Gillis for preliminary computations, and the Atlantic Computational Excellence Network (ACEnet) for providing computational resources. ACEnet is the regional high performance computing consortium for universities in Atlantic Canada and is funded by the Canada Foundation for Innovation (CFI), the Atlantic Canada Opportunities Agency (ACOA), and the provinces of Nova Scotia, New Brunswick, and Newfoundland & Labrador.

REFERENCES

[1] K. Grossmann. Auxin herbicides: current status of mechanism and mode of action. *Pest Manag. Sci.* **2010**, *66*, 113.
[2] K. Pahan. Biomedicine & diseases: review. Lipid-lowering drugs. *Cell. Mol. Life Sci.* **2006**, *63*, 1165.
[3] R. R. Patel, M. P. Mehta. Targeted therapy for brain metastases: improving the therapeutic ratio. *Clin. Cancer Res.* **2007**, *13*, 1675.
[4] A. J. Ramirez, M. A. Mottaleb, B. W. Brooks, C. K. Chambliss. Analysis of pharmaceuticals in fish using liquid chromatography-tandem mass spectrometry. *Anal. Chem.* **2007**, *79*, 3155.
[5] S. Bogialli, R. Curini, A. Di Corcia, A. Laganà, A. Stabile, E. Sturchio. Development of a multiresidue method for analyzing herbicide and fungicide residues in bovine milk based on solid-phase extraction and liquid chromatography–tandem mass spectrometry. *J. Chromatogr. A* **2006**, *1102*, 1.
[6] M. Thevis, O. Krug, W. Schänzer. Mass spectrometric characterization of efaproxiral (RSR13) and its implementation into doping controls using liquid chromatography–atmospheric pressure ionization-tandem mass spectrometry. *J. Mass Spectrom.* **2006**, *41*, 332.
[7] M. J. M. Bueno, A. Agüera, M. J. Gómez, M. D. Hernando, J. F. García-Reyes, A. R. Fernández-Alba. Application of liquid chromatography/quadrupole-linear ion trap mass spectrometry and time-of-flight mass spectrometry to the determination of pharmaceuticals and related contaminants in wastewater. *Anal. Chem.* **2007**, *79*, 9372.
[8] M. Gros, M. Petrović, D. Barceló. Development of a multi-residue analytical methodology based on liquid chromatography–tandem mass spectrometry (LC–MS/MS) for screening and trace level determination of pharmaceuticals in surface and wastewaters. *Talanta* **2006**, *70*, 678.
[9] D. Löffler, T. A. Ternes. Determination of acidic pharmaceuticals, antibiotics and ivermectin in river sediment using liquid chromatography–tandem mass spectrometry. *J. Chromatogr. A* **2003**, *1021*, 133.
[10] X.-S. Miao, B. G. Koenig, C. D. Metcalfe. Analysis of acidic drugs in the effluents of sewage treatment plants using liquid chromatography–electrospray ionization tandem mass spectrometry. *J. Chromatogr. A* **2002**, *952*, 139.
[11] X. Song, W. L. Budde. Determination of chlorinated acid herbicides and related compounds in water by capillary electrophoresis–electrospray negative ion mass spectrometry. *J. Chromatogr. A* **1998**, *829*, 327.
[12] D. Schröder, N. Golberg, W. Zummack, H. Schwarz, J. C. Poutsma, R. R. Squires. Generation of α-acetolactone and the acetoxyl diradical XCH_2COOX in the gas phase. *Int. J. Mass Spectrom. Ion Processes* **1997**, *165/166*, 71.
[13] S. T. Graul, R. R. Squires. Collisional activation of intramolecular nucleophilic displacement reactions: the formation of acetolactone from dissociation of α-haloacetate negative ions. *Int. J. Mass Spectrom. Ion Processes* **1990**, *100*, 785.
[14] C. F. Rodriquez, I. H. Williams. *Ab initio* theoretical investigation of the mechanism for α-lactone formation from α-halocarboxylates: leaving group, substituent, solvent and isotope effects. *J. Chem. Soc. Perkin Trans. 2* **1997**, 959.
[15] D. Antolovic, V. J. Shiner, E. R. Davidson. Theoretical study of α-lactone, acetoxyl diradical, and the gas-phase dissociation of the chloroacetate anion. *J. Am. Chem. Soc.* **1988**, *110*, 1375.
[16] Y. Li, Y. Chai, L. Wang, Y. Pan, S. Zeng, C. Sun. Gas-phase Smiles rearrangement reactions of deprotonated *N*-phenylbenzamides studied by electrospray ionization tandem mass spectrometry. *Rapid Commun. Mass Spectrom.* **2015**, *29*, 864.

[17] T. Wang, N. M. M. Nibbering, J. H. Bowie. The gas phase Smiles rearrangement of anions $PhO(CH_2)_nO^-$ (n = 2–4). A joint theoretical and experimental approach. *Org. Biomol. Chem.* **2010**, *8*, 4080.
[18] F. Wang. Collision-induced gas-phase Smiles rearrangement in phenoxy-N-phenylacetamide derivatives. *Rapid Commun. Mass Spectrom.* **2006**, *20*, 1820.
[19] P. C. H. Eichinger, J. H. Bowie. The gas-phase Smiles rearrangement. The effect of ring substitution. An ^{18}O labelling study. *Org. Mass Spectrom.* **1992**, *27*, 995.
[20] P. C. H. Eichinger, J. H. Bowie, R. N. Hayes. The gas-phase Smiles rearrangement: a heavy atom labeling study. *J. Am. Chem. Soc.* **1989**, *111*, 4224.
[21] T. E. Tovstiga, E. A. L. Gillis, J. S. Grossert, R. L. White. Characterization of multiple fragmentation pathways initiated by collision-induced dissociation of multifunctional anions formed by deprotonation of 2-nitrobenzenesulfonylglycine. *J. Mass Spectrom.* **2014**, *49*, 168.
[22] R. Visser, W. P. M. Maas, N. M. M. Nibbering. Collision-induced dissociation reactions of *o*-, *m*-, *p*-methoxyphenyl anions in the gas phase. *Recl. Trav. Chim. Pays-Bas* **1990**, *109*, 248.
[23] L. Sleno, R. F. Staack, E. Varesio, G. Hopfgartner. Investigating the *in vitro* metabolism of fipexide: characterization of reactive metabolites using liquid chromatography/mass spectrometry. *Rapid Commun. Mass Spectrom.* **2007**, *21*, 2301.
[24] L. E. Greene, J. S. Grossert, R. L. White. Correlations of ion structure with multiple fragmentation pathways arising from collision-induced dissociations of selected α-hydroxycarboxylic acid anions. *J. Mass Spectrom.* **2013**, *48*, 312.
[25] S. T. Graul, R. R. Squires. Generation of alkyl carbanions in the gas phase. *J. Am. Chem. Soc.* **1990**, *112*, 2506.
[26] M. K. Kumar, B. Sateesh, S. Prabhakar, G. N. Sastry, M. Vairamani. Generation of regiospecific carbanions under electrospray ionisation conditions and their selectivity in ion-molecule reactions with CO_2. *Rapid Commun. Mass Spectrom.* **2006**, *20*, 987.
[27] T. Bieńkowski, W. Danikiewicz. Generation and reactions of substituted phenide anions in an electrospray triple quadrupole mass spectrometer. *Rapid Commun. Mass Spectrom.* **2003**, *17*, 697.
[28] R. R. Squires. Gas-phase carbanion chemistry. *Acc. Chem. Res.* **1992**, *25*, 461.
[29] D. R. Reed, S. R. Kass, K. R. Mondanaro, W. P. Dailey. Formation of a 1-bicyclo[1.1.1]pentyl anion and an experimental determination of the acidity and C–H bond dissociation energy of 3-tert-butylbicyclo[1.1.1]pentane. *J. Am. Chem. Soc.* **2002**, *124*, 2790.
[30] E. A. L. Gillis, J. S. Grossert, R. L. White. Rearrangements leading to fragmentations of hydrocinnamate and analogous nitrogen-containing anions upon collision-induced dissociation. *J. Am. Soc. Mass Spectrom.* **2014**, *25*, 388.
[31] D. W. Manley, R. T. McBurney, P. Miller, J. C. Walton, A. Mills, C. O'Rourke. Titania-promoted carboxylic acid alkylations of alkenes and cascade addition–cyclizations. *J. Org. Chem.* **2014**, *79*, 1386.
[32] http://www.dal.ca/faculty/science/chemistry/research/dalchem-mass-spectrometry-laboratory.html (accessed August 11, 2015).
[33] M. J. Frisch, G. W. Trucks, H. B. Schlegel, G. E. Scuseria, M. A. Robb, J. R. Cheeseman, G. Scalmani, V. Barone, B. Mennucci, G. A. Petersson, H. Nakatsuji, M. Caricato, X. Li, H. P. Hratchian, A. F. Izmaylov, J. Bloino, G. Zheng, J. L. Sonnenberg, M. Hada, M. Ehara, K. Toyota, R. Fukuda, J. Hasegawa, M. Ishida, T. Nakajima, Y. Honda, O. Kitao, H. Nakai, T. Vreven, J. A. Montgomery Jr., J. E. Peralta, F. Ogliaro, M. Bearpark, J. J. Heyd, E. Brothers, K. N. Kudin, V. N. Staroverov, T. Keith, R. Kobayashi, J. Normand, K. Raghavachari, A. Rendell, J. C. Burant, S. S. Iyengar, J. Tomasi, M. Cossi, N. Rega, J. M. Millam, M. Klene, J. E. Knox, J. B. Cross, V. Bakken, C. Adamo, J. Jaramillo, R. Gomperts, R. E. Stratmann, O. Yazyev, A. J. Austin, R. Cammi, C. Pomelli, J. W. Ochterski, R. L. Martin, K. Morokuma, V. G. Zakrzewski, G. A. Voth, P. Salvador, J. J. Dannenberg, S. Dapprich, A. D. Daniels, O. Farkas, J. B. Foresman, J. V. Ortiz, J. Cioslowski, D. J. Fox. *Gaussian 09, Revision D.01*. Gaussian, Inc., Wallingford, CT, **2013**.
[34] A. D. Becke. Density-functional thermochemistry. III. The role of exact exchange. *J. Chem. Phys.* **1993**, *98*, 5648.
[35] A. D. Becke. Density-functional exchange-energy approximation with correct asymptotic behavior. *Phys. Rev. A: At., Mol., Opt. Phys.* **1988**, *38*, 3098.
[36] C. Lee, W. Yang, R. G. Parr. Development of the Colle-Salvetti correlation-energy formula into a functional of the electron density. *Phys. Rev. B: Condens. Matter Mater. Phys.* **1988**, *37*, 785.
[37] R. W. Binkley, M. J. S. Tevesz, W. Winnik. Reactions of phenoxide ion in the gas phase. *J. Org. Chem.* **1992**, *57*, 5507.
[38] N. Chéron, D. Jacquemin, P. Fleurat-Lessard. A qualitative failure of B3LYP for textbook organic reactions. *Phys. Chem. Chem. Phys.* **2012**, *14*, 7170.
[39] Y. Zhao, D. G. Truhlar. The M06 suite of density functionals for main group thermochemistry, thermochemical kinetics, noncovalent interactions, excited states, and transition elements: two new functionals and systematic testing of four M06-class functionals and 12 other functionals. *Theor. Chem. Acc.* **2008**, *120*, 215.
[40] J.-D. Chai, M. Head-Gordon. Systematic optimization of long-range corrected hybrid density functionals. *J. Chem. Phys.* **2008**, *128*, 084106/1–15.
[41] J.-D. Chai, M. Head-Gordon. Long-range corrected hybrid density functionals with damped atom–atom dispersion corrections. *Phys. Chem. Chem. Phys.* **2008**, *10*, 6615.
[42] S. T. Graul, R. R. Squires. Gas-phase acidities derived from threshold energies for activated reactions. *J. Am. Chem. Soc.* **1990**, *112*, 2517.
[43] K. B. Herath, C. S. Weisbecker, S. B. Singh, A. B. Attygalle. Circumambulatory movement of negative charge ("ring walk") during gas-phase dissociation of 2,3,4-trimethoxybenzoate anion. *J. Org. Chem.* **2014**, *79*, 4378.
[44] P. C. H. Eichinger, J. H. Bowie, R. N. Hayes. Stable negative-ion isomers in the gas phase. $C_7H_7O^-$ species. *Aust. J. Chem.* **1989**, *42*, 865.
[45] J. C. Kleingeld, N. M. M. Nibbering. Hydrogen/deuterium exchange in gas phase reactions of anions with some alkyl phenyl ethers. *Tetrahedron* **1983**, *39*, 4193.
[46] M. J. Raftery, J. H. Bowie, J. C. Sheldon. Collision-induced dissociations of aryl-substituted alkoxide ions. Losses of dihydrogen and rearrangement processes. *J. Chem. Soc. Perkin Trans. 2* **1988**, 563.
[47] B. Kanawati, P. Schmitt-Kopplin. Exploring rearrangements along the fragmentation of glutaric acid negative ion: a combined experimental and theoretical study. *Rapid Commun. Mass Spectrom.* **2010**, *24*, 1198.
[48] L. B. Reeks, P. C. H. Eichinger, J. H. Bowie. *ortho*-Rearrangements of *o*-alkylphenoxide anions. *Rapid Commun. Mass Spectrom.* **1993**, *7*, 286.

SUPPORTING INFORMATION

Additional supporting information may be found in the online version of this article at the publisher's website.

